Pergamon PII: S0038–092X(02)00027–0
Solar Energy Vol. 72, No. 6, pp. 473–492, 2002

0038-092X/02/$ - see front matter
www.elsevier.com/locate/solener

IMPLEMENTING THE PARTIAL DAYLIGHT FACTOR METHOD UNDER A SCANNING SKY SIMULATOR

LAURENT MICHEL† and JEAN-LOUIS SCARTEZZINI
Solar Energy and Building Physics Laboratory (LESO-PB), Swiss Federal Institute of Technology in Lausanne (EPFL), CH-1015 Lausanne, Switzerland

Received 30 April 2001; revised version accepted 17 April 2002

Communicated by VOLKER WITTWER

Abstract—Architects need support for the evaluation of the daylighting performance of their buildings. As experimental tools, sky simulators, used in conjunction with scale models, allow a concrete and intuitive approach to the problem. Yet conventional artificial skies and their measurement technology are of limited use, because they are usually not able to evaluate building performance under a non-standard sky luminance distribution (CIE sky models). The Partial Daylight Factor (PDF) method presented in this paper addresses this problem. It is applied to a scanning sky simulator in conjunction with a methodology of experimental research (experimental plans of Hadamard). Scale model experimental simulations carried out with the scanning sky simulator and the PDF method offer an evaluation of the daylighting performance of a building for any luminous configuration of the sky vault. Coupled to a climatic database, they allow an evaluation of daylighting performance indicators such as daylight sufficiency and average or cumulated illuminance for all types of overcast, intermediate and clear skies, including CIE standard models. Moreover, new concepts, such as the Partial Illuminance Factor (PIF), allow a better knowledge and comprehension of the daylighting strategy.

1. INTRODUCTION

Several decades ago, the International Commission of Illumination (Commission Internationale de l'Eclairage, CIE) officially adopted the Daylight Factor (DF) method (CIE16, 1970). As this method is easy to implement, it is largely used, in particular within the framework of experimental simulations under mirror or dome sky simulators. These simulators are well adapted to the task because they usually reproduce a standard luminance distribution defined for an overcast sky by the CIE (Moon and Spencer), which corresponds to that assumed by the DF method. Simulations therefore comply with the standard performance assessment method.

Unfortunately, the DF varies considerably with the sky vault luminance distribution, even when there is no direct component of daylight (sun rays): Tregenza (1980), for instance, reports ratios of approximately 1:5 between the lowest and highest values observed for a given point within a room. As dome or mirror type sky simulators are not able to reproduce luminance distributions other than a standard overcast sky, it is impossible to reproduce the real dynamic behaviour of daylight in buildings with these devices, in particular under a clear sky. This constitutes an unquestionable handicap in the development of new daylighting systems or strategies. In the experimental context, it is also important to say that daylight performance evaluations within scale models show a 10–55% divergence with full-scale measurements (Cannon-Brookes, 1997). This does not mean that scale model simulations are not appropriate for the evaluation of the daylight performance of a building, but it gives some idea of the error margin. Of course, such divergences should be reduced, but they do not counterbalance the interest of scale model simulation in practice.

This paper describes a new approach, the Partial Daylight Factor method (PDF), which overcomes the difficulties described above. Implemented in conjunction with a novel generation of sky simulators (scanning sky simulator), the method allows studies and a better understanding of daylight penetration into buildings, for any sky luminance distribution, including monitored sky luminance data.

2. PRINCIPLES OF THE PARTIAL DAYLIGHT FACTOR METHOD

Several methods have been proposed for the

†Author to whom correspondence should be addressed. Tel.: +41-21-693-4545; fax: +41-21-693-2722; e-mail: leso-pb@epfl.ch

assessment of daylight performance in buildings, in particular:

- the Daylight Factor method (CIE16, 1970)
- the Daylight Coefficients method (Tregenza and Waters, 1983; Tregenza, 1989)
- the Integration of Directional Coefficients (IDC) (Papamichael and Beltran, 1993)
- the Frequency Method (Dumortier, 1995)

As stated above, the first method can be considered as a standard procedure for daylight performance assessment of buildings, whose use should be restricted, however, to a specific type of overcast sky. Tregenza and Waters overcame this drawback by proposing the Daylight Coefficient method: the use of a sky vault discretisation which is not in accordance with the format employed for monitoring sky luminance distribution at the international level limits; however, the practicability of this novel approach is useful. The IDC method suggested by Papamichael and Beltran was apparently inspired by the work of Tregenza: it suffers from the same drawback and focuses on single building apertures. More recently, Dumortier followed a similar way, suggesting a method able to generate illuminance frequency distributions and offering alternatives to the conventional daylighting performance indicators.

Table 1 gives a short overview of the main features of these methods; more details can be found in the publications referred to.

The partial daylight factor (PDF) method pursues similar objectives as the methods described above. It allows the assessment of several daylighting performance indicators, such as work plane illuminance, daylighting sufficiency and illuminance threshold probabilities.

The subdivision of the sky vault into 145 luminous zones adopted by the International Daylighting Monitoring Programme (IDMP) in accordance with Tregenza (1987) is used to define Partial Daylight Factors (PDF) that describe the daylight contribution of each zone to the illuminance of a given point in a building. Fig. 1 illustrates the principle of the method, presented in detail in Michel (1999).

If the 145 PDF values D_j $(1 \leq j \leq 145)$ are known, it is possible to determine global values by adding the contributions weighted by the corresponding sky luminance of zone j: thus, we can determine the illuminance at the considered point for any type of sky luminance distribution (overcast, intermediate or clear sky with direct sunlight component).

The following daylight performance indicators can also be assessed using Partial Daylight Factors:

- Illuminance Factor (IF)
- Partial Illuminance Factor (PIF)
- Temporal Fraction of Satisfaction (TFS)

The way these indicators can be determined using PDFs is described below.

2.1. *Definition of Partial Daylight Factor (PDF)*

The Partial Daylight Factor D_j at a given point

Table 1. Main features, advantages and disadvantages of different daylight performance assessment methods of buildings

Method	Definition	Advantages	Disadvantages
Daylight factor (CIE16, 1970)	Ratio of the work-plane horizontal illuminance at a given point and the global external horizontal illuminance under a CIE unobstructed overcast sky (Moon and Spencer distribution)	–easy implementation –low cost standard equipment –common use –can be used on site	–sensitive to type of the cloud cover –cannot be used to evaluate performances for other types of sky than CIE overcast sky
Daylight Coefficient (Tregenza and Waters, 1983) (Tregenza, 1989)	Daylight coefficients defined for each elementary portion of sky vault.	–illuminance can be calculated inside a building for any sky distribution	–sky vault geometry not in accordance with the IDMP format
Integration of Directional Coefficients (IDC) (Papamichael and Beltran, 1993)	Similar definition, but centred on a single aperture; gives four contributions of light in different directions (direct/diffuse, sky/ground)	–illuminance can be calculated inside a building for any sky distribution	–sky vault geometry not in accordance with the IDMP format
Frequency Method (Dumortier, 1995)	Distinguishes between ‘optical’ and ‘climatic’ calculation.	–possibility to evaluate the luminous performance of a building for all monitored data –possibility to generate a distribution frequency curve of illuminance	–sky vault geometry not in accordance with the IDMP format

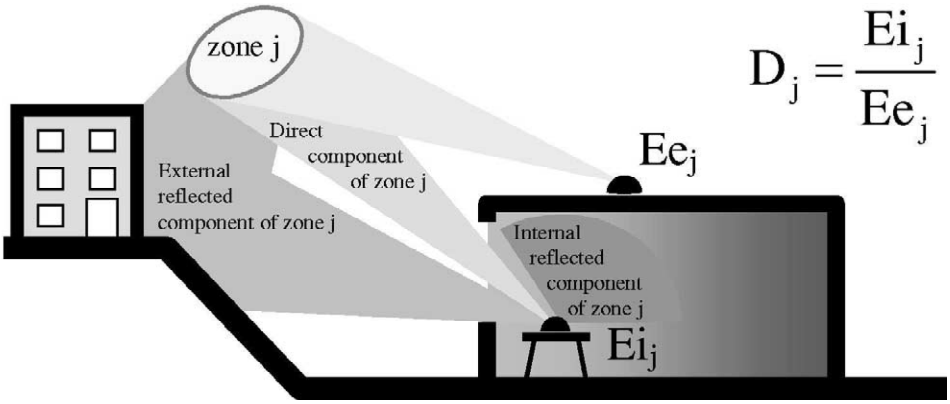

Fig. 1. Principles of the Partial Daylight Factor method where $D_j = Ei_j/Ee_j$ is the Partial Daylight Factor due to luminous zone j of the sky vault.

(e.g. the work desk surface) due to luminous zone j, is defined by:

$$D_j = \frac{Ei_j}{Ee_j} [-] \tag{1}$$

with Ei_j [Lx], contribution of zone j to the horizontal illuminance at a given point inside a building; Ee_j [Lx], contribution of zone j to the external global horizontal illuminance.

It is possible to express the external partial illuminance Ee_j according to the luminance L_j associated to zone j using the equation:

$$Ee_j = L_j \cdot \Omega_j \cdot \sin \eta_j \tag{2}$$

with L_j [cd/m^2], average luminance of zone j; Ω_j [sr], apparent solid angle of zone j; η_j [rad], angular altitude above the horizon of zone j centre.

2.2. Determining the work plane illuminance

The external horizontal illuminance Ee_0^{iso} due to an isotropic sky luminance distribution can first be determined under any sky simulator that reproduces the ($N = 145$) luminous zones defined by Tregenza (see Section 3) using the following expression, with an equal luminance (isotropic sky):

$$Ee_0^{\text{iso}} = \sum_{j=1}^{N} Ee_j^{\text{iso}} \tag{3}$$

where Ee_j^{iso} [Lx] is the contribution of each zone j to the external illuminance of an isotropic sky.

The global external horizontal illuminance observed for a given sky luminance distribution L_j ($1 \leq j \leq 145$) is given by:

$$Ee_0 = \sum_{j=1}^{N} Ee_j^{\text{iso}} \cdot \frac{L_j}{L^{\text{iso}}} \tag{4}$$

The work plane horizontal illuminance observed at a given point in a building can be expressed as:

$$Ei_0 = \sum_{j=1}^{N} Ei_j \tag{5}$$

Using the Partial Daylight Factors D_j (see Eq. (1)), this equation can be replaced by:

$$Ei_0 = \sum_{j=1}^{N} D_j \cdot Ee_j = \sum_{j=1}^{N} D_j \cdot Ee_j^{\text{iso}} \cdot \frac{L_j}{L^{\text{iso}}} \tag{6}$$

This allows determining the illuminance Ei_0 at a given point in a building for any sky luminance distribution L_j ($1 \leq j \leq 145$) on the basis of a rather conventional experiment carried out under an isotropic sky luminance distribution.

2.3. Determining the Illuminance Factor (IF) and the Daylight Factor (DF)

As the International Commission on Illumination (CIE16, 1970) defines the Daylight Factor (DF) at a given point for a standardised overcast unobstructed sky (see Eq. (8)), the Illuminance Factor (IF) is used instead to designate the ratio Ei_0/Ee_0 for any type of sky. Following Eqs. (4) and (6) this factor can be expressed as follows:

$$\text{IF} = \frac{Ei_0}{Ee_0} = \frac{\sum_{j=1}^{N} D_j \cdot Ee_j^{\text{iso}} \cdot \frac{L_j}{L^{\text{iso}}}}{\sum_{j=1}^{N} Ee_j^{\text{iso}} \cdot \frac{L_j}{L^{\text{iso}}}} = \frac{\sum_{j=1}^{N} D_j \cdot Ee_j^{\text{iso}} \cdot L_j}{\sum_{j=1}^{N} Ee_j^{\text{iso}} \cdot L_j} \tag{7}$$

which can be considered as a generalisation of the Daylight Factor method for non CIE standard overcast skies. In consequence, both factors are equal when L_j $(1 \le j \le 145)$ follows the Moon and Spencer distribution given in (8):

$$\mathrm{DF} = \mathrm{IF} \quad \text{when} \quad L_j = L_z \cdot \frac{1 + 2 \cdot \sin \eta_j}{3} \tag{8}$$

with L_z [cd/m^2], sky luminance at zenith; η_j [rad], angular altitude above horizon of zone j centre.

2.4. Definition of the Partial Illuminance Factor (PIF)

The Partial Illuminance Factor (PIF) is a ratio expressed in [%] that is proportional to the contribution of each sky zone j to the work plane illuminance Ei_0 at a given point inside a building. It depends on the sky luminance distribution L_j and is expressed by the following equation for a given location in a building:

$$\mathrm{PIF}_j = \frac{Ei_j}{\sum_{k=1}^{N} Ei_k} = \frac{Ei_j}{Ei_0} \, [-]$$

$$\text{with} \quad \sum_{j=1}^{N} \mathrm{PIF}_j = 1 \; (N = 145) \tag{9}$$

If not specified otherwise, we will consider the sky luminance distribution as isotropic and, for reasons of simplicity, will omit it in the notation of the PIF.

The PIF allows a better understanding of direct and diffuse daylight component penetration into a considered building: high PIF_j values for a certain luminous zone j indicate a significant contribution of this zone to the daylighting of a given point in a building

2.5. Definition of Temporal Fraction of Satisfaction (TFS)

The TFS is the fraction of working hours during which the work plane illuminance satisfies a defined lighting criterion. The number and the nature of such criteria can vary; however, three basic cases can be distinguished:

1. $\mathrm{TFS}^{\min}$ in the case $Ei_0 > E_0^{\min}$: Work plane illuminance Ei_0 must be larger than a minimal required illuminance value $E_0^{\min}$, defined for daylight sufficiency (e.g.: 300–500 lux for a horizontal work plane illuminance for reading/writing tasks)
2. $\mathrm{TFS}^{\max}$ in the case $Ei_0 < E_0^{\max}$: Work plane illuminance Ei_0 must be lower than a given maximal value $E_0^{\max}$, as an excessive illuminance on the work plane may cause glare.
3. $\mathrm{TFS}^{\min/\max}$ in the case $E_0^{\min} < Ei_0 < E_0^{\max}$: Work plane illuminance Ei_0 must be included between a minimal and a maximal value, which is the conjunction of the two preceding criteria.

Fig. 2 graphically illustrates the three criteria above. The time of utilisation of a daylit office is generally defined as the usual daily work hours.

The TFS can be determined experimentally using a scale model of a building, providing that IDMP sky luminance and illuminance statistical data are available for the considered building site. Such data comprise hourly values of global horizontal illuminance Ee_0 together with 145 sky luminance values L_j that describe the sky luminance distribution, including the zones that match the sun path.

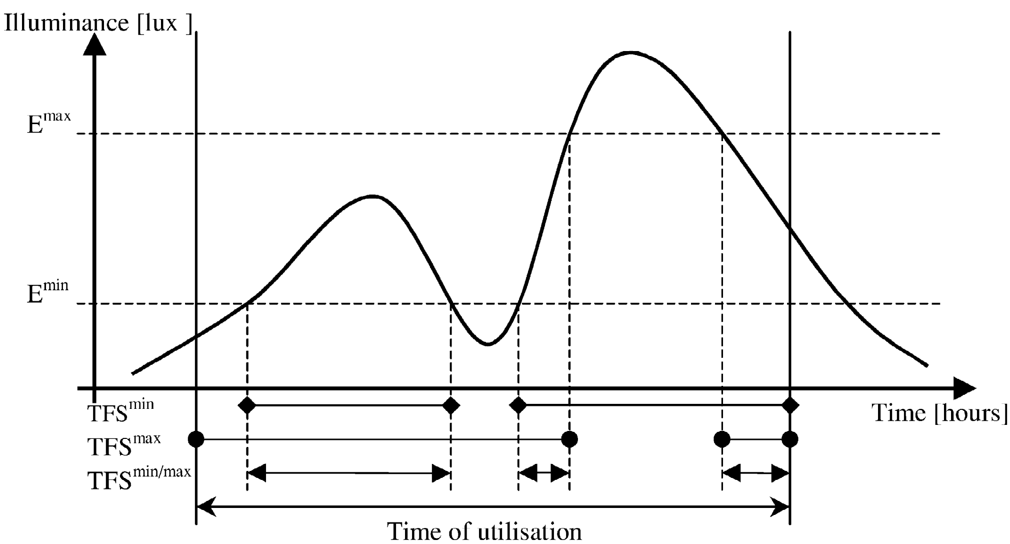

Fig. 2. Criteria used to define the Temporal Fraction of Satisfaction (TFS).

3. EXPERIMENTAL ASSESSMENT OF PDF

Partial Daylight Factors can be experimentally assessed using sky simulators that reproduce the IDMP luminance distribution, such as the scanning sky simulator designed and built at the EPFL (Michel *et al*., 1995); this simulator draws extensive daylight performance assessment capabilities from the PDF method. In order to implement the method experimentally, work is carried out in two stages:

- Measurement stage: A scale model, even a complex one that involves several window openings and daylighting systems (the PDF method does not impose the same restrictions as the IDC method), is placed under the scanning sky simulator; the measurement procedure described below in Section 3.1 is applied.
- Calculation stage: The data from the measurement stage are treated as described in Section 3.2. A dedicated piece of software allows evaluating the daylighting performance of a building per room based on:
  - Illuminance Factors for all types of sky (including CIE Daylight Factors)
  - daylight availability profiles
  - Temporal Fraction of Satisfaction profiles
  - contributions of the different sky zones to the internal illuminance
  - cumulated indoor illuminance at a given point.

The scanning sky simulator (see Fig. 3) allows separate driving of the 145 luminous zones of the hemisphere (see Fig. 4) defined in Tregenza's (1987) model and adopted by the International Daylight Monitoring Program (IDMP): the device can therefore be used to experimentally assess the PDF of a given building according to Eq. (1).

To determine the 145 PDF values, a standard approach would be to switch on the different luminous zones corresponding to Tregenza's model, one by one. This trivial experiment, probably easier to understand intuitively, has the disadvantage that the illuminance due to each single light source is not very strong, which leads to a low signal to noise ratio and a relatively high error margin.

A more appropriate approach is the one based on a Hadamard experimental design (see Appendix A for more details), which is possible because the luminance values of the 25 light sources of the scanning sky simulator (see Fig. 5) are physically independent and show a linear response. It presents the following advantages:

- the Hadamard experimental plan, which in this case consists of 28 experiments, reduces the experimental error by a factor equivalent to $\sqrt{28} = 5.3$
- at least 12 light sources are lit simultaneously

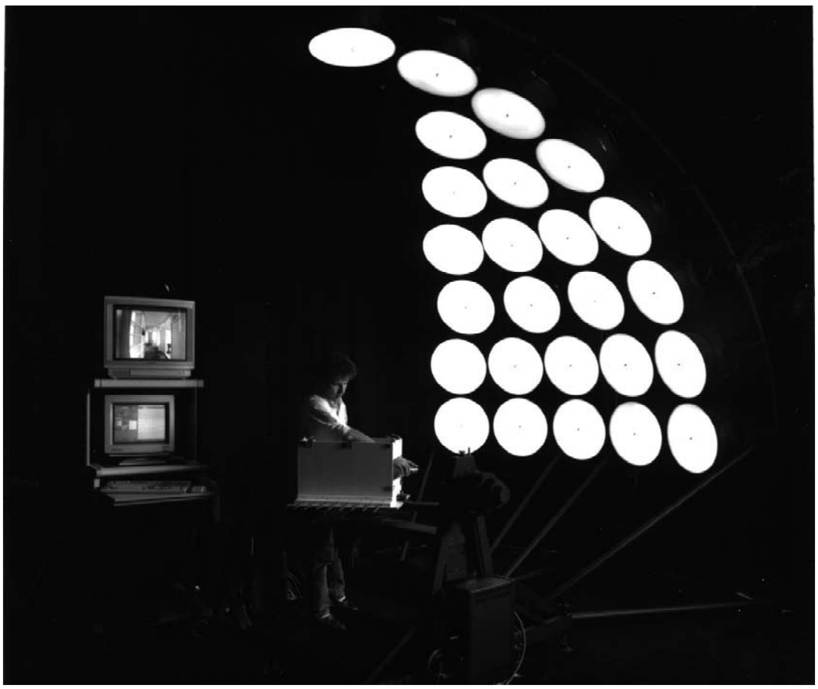

Fig. 3. View of the scanning sky simulator. The scale model is placed on an automated rotating support at the centre of the sky dome.

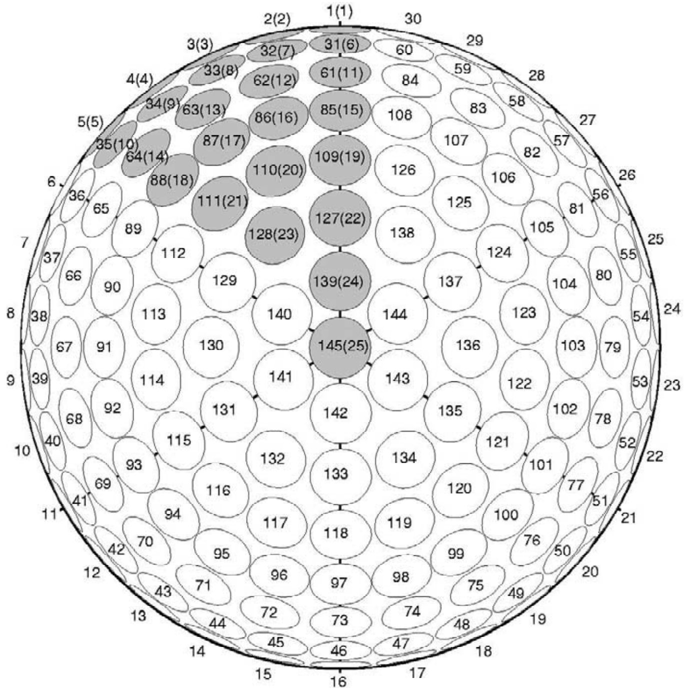

Zone Number	Altitude of band centre [°]	Azimuth increment [°]
1-30	6	12
31-60	18	12
61-84	30	15
85-108	42	15
109-126	54	20
127-138	66	30
139-144	78	60
145	90	-

Fig. 4. Configuration of the scanning sky simulator according to Tregenza's (1987) model. Only the grey zones (numbering in brackets) were physically built (one sixth of a 5 m diameter hemisphere). The full vault is reproduced through six (60°) rotations of the scale model.

(see Table 2), which leads to a better signal to noise ratio.

3.1. Measurement procedure

The configuration of the light sources, that correspond to each experimental state (+1) and (−1) of the Hadamard matrix, can be chosen arbitrarily. To achieve the best possible accuracy, assuming a linear relation, two extreme states of lighting are used:

- level (−1) equivalent to 'light off'
- level (+1) equivalent to 'full power on'

As shown in Appendix A, the number of experiments has to be a multiple of 4. Thus, to determine the 25 PDFs of each light source of the scanning artificial sky, it is necessary to use a Hadamard's matrix that corresponds to $(4\times7)=28$ experiments. Two factors are supernumerary: they are in consequence not assigned to any lighting fixture.

Many publications describe how to construct a Hadamard's matrix. The one used here for 28 experiments (see Table 2) is given in Plackett and Burman (1946). Each column corresponds to one of the light sources of the scanning sky simulator and each line corresponds to one artificial sky luminous configuration. The first experiment (line no. 1 of Table 2) is illustrated in Fig. 5.

The principle of the scanning sky simulator is to reproduce six sectors of the sky vault (Michel *et al*., 1995). Consequently, Hadamard's plan of 28 experiments is repeated six times, each time after a 60° rotation of the scale model. On the whole, the automated procedure of the scanning sky simulator performs in this case $(28\times6)=168$ measurements, which take about 20 minutes.

The 168 data are stored for each of the ten

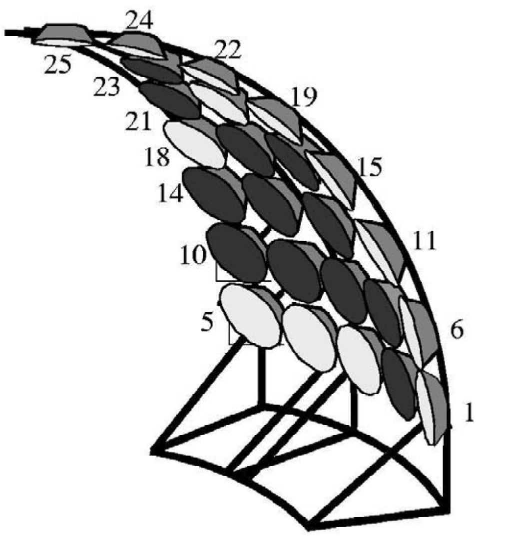

Fig. 5. Sketch of the first artificial sky configuration (with light source numeration) according to the Hadamard experimental design.

Table 2. Description of the state of the 25 luminous disks during the 28 experiments of Hadamard's plan. The first experiment (line no. 1) is illustrated in Fig. 5: (+1) means light source 'on', (−1) means light source 'off'

Experiment number	State of the 25 luminous disks of the scanning sky simulator (numbers correspond to numeration in brackets of Fig. 4)																									Non-assigned	
	1	2	3	4	5	6	7	8	9	10	11	12	13	14	15	16	17	18	19	20	21	22	23	24	25		
1	+1	−1	+1	+1	+1	+1	−1	−1	−1	−1	+1	−1	−1	−1	+1	−1	−1	+1	+1	+1	−1	+1	−1	+1	+1	−1	+1
2	+1	+1	−1	+1	+1	+1	−1	−1	−1	−1	−1	+1	+1	−1	−1	+1	−1	−1	−1	+1	+1	+1	+1	−1	+1	+1	−1
3	−1	+1	+1	+1	+1	+1	−1	−1	−1	+1	−1	−1	−1	+1	−1	−1	+1	−1	+1	−1	+1	−1	+1	+1	−1	+1	+1
4	−1	−1	−1	+1	−1	+1	+1	+1	+1	−1	−1	+1	−1	+1	−1	−1	−1	+1	+1	−1	+1	+1	+1	−1	+1	−1	+1
5	−1	−1	−1	+1	+1	−1	+1	+1	+1	+1	−1	−1	−1	−1	+1	+1	−1	−1	+1	+1	−1	−1	+1	+1	+1	+1	−1
6	−1	−1	−1	−1	+1	+1	+1	+1	+1	−1	+1	−1	+1	−1	−1	−1	+1	−1	−1	+1	+1	+1	−1	+1	−1	+1	+1
7	+1	+1	+1	−1	−1	−1	+1	−1	+1	−1	−1	+1	−1	−1	+1	−1	+1	−1	+1	−1	+1	+1	−1	+1	+1	+1	−1
8	+1	+1	+1	−1	−1	−1	+1	+1	−1	+1	−1	−1	+1	−1	−1	−1	−1	+1	+1	+1	−1	+1	+1	−1	−1	+1	+1
9	+1	+1	+1	−1	−1	−1	−1	+1	+1	−1	+1	−1	−1	+1	−1	+1	−1	−1	−1	+1	+1	−1	+1	+1	+1	−1	+1
10	+1	+1	−1	+1	−1	+1	+1	−1	+1	+1	−1	+1	+1	+1	+1	−1	−1	−1	−1	+1	−1	−1	−1	+1	−1	−1	+1
11	−1	+1	+1	+1	+1	−1	+1	+1	−1	+1	+1	−1	+1	+1	+1	−1	−1	−1	−1	−1	+1	+1	−1	−1	+1	−1	−1
12	+1	−1	+1	−1	+1	+1	−1	+1	+1	−1	+1	+1	+1	+1	+1	−1	−1	−1	+1	−1	−1	−1	+1	−1	−1	+1	−1
13	+1	−1	+1	+1	+1	−1	+1	−1	+1	−1	−1	−1	+1	−1	+1	+1	+1	+1	−1	−1	+1	−1	+1	−1	−1	−1	+1
14	+1	+1	−1	−1	+1	+1	+1	+1	−1	−1	−1	−1	+1	+1	−1	+1	+1	+1	+1	−1	−1	−1	−1	+1	+1	−1	−1
15	−1	+1	+1	+1	−1	+1	−1	+1	+1	−1	−1	−1	−1	+1	+1	+1	+1	+1	−1	+1	−1	+1	−1	−1	−1	+1	−1
16	+1	−1	+1	+1	−1	+1	+1	+1	−1	+1	+1	+1	−1	−1	−1	+1	−1	+1	−1	−1	+1	−1	−1	+1	−1	+1	−1
17	+1	+1	−1	+1	+1	−1	−1	+1	+1	+1	+1	+1	−1	−1	−1	+1	+1	−1	+1	−1	−1	+1	−1	−1	−1	−1	+1
18	−1	+1	+1	−1	+1	+1	+1	−1	+1	+1	+1	+1	−1	−1	−1	−1	+1	+1	−1	+1	−1	−1	+1	−1	+1	−1	−1
19	−1	+1	−1	−1	−1	+1	−1	−1	+1	+1	+1	−1	+1	−1	+1	+1	−1	+1	+1	−1	+1	+1	+1	+1	−1	−1	−1
20	−1	−1	+1	+1	−1	−1	+1	−1	−1	−1	+1	+1	+1	+1	−1	+1	+1	−1	+1	+1	−1	+1	+1	+1	−1	−1	−1
21	+1	−1	−1	−1	+1	−1	−1	+1	−1	+1	−1	+1	−1	+1	+1	−1	+1	+1	−1	+1	+1	+1	+1	+1	−1	−1	−1
22	−1	−1	+1	−1	+1	−1	−1	−1	+1	+1	−1	+1	+1	+1	−1	+1	−1	+1	−1	−1	−1	+1	−1	+1	+1	+1	+1
23	+1	−1	−1	−1	−1	+1	+1	−1	−1	+1	+1	−1	−1	+1	+1	+1	+1	−1	−1	−1	−1	+1	+1	−1	+1	+1	+1
24	−1	+1	−1	+1	−1	−1	−1	+1	−1	−1	+1	+1	+1	−1	+1	−1	+1	+1	−1	−1	−1	−1	+1	+1	+1	+1	+1
25	−1	−1	+1	−1	−1	+1	−1	+1	−1	+1	−1	+1	+1	−1	+1	+1	+1	−1	+1	+1	+1	−1	−1	−1	+1	−1	+1
26	+1	−1	−1	+1	−1	−1	−1	−1	+1	+1	+1	−1	+1	+1	−1	−1	+1	+1	+1	+1	+1	−1	−1	−1	+1	+1	−1
27	−1	+1	−1	−1	+1	−1	+1	−1	−1	−1	+1	+1	−1	+1	+1	+1	−1	+1	+1	+1	+1	−1	−1	−1	−1	+1	+1
28	−1	−1	−1	−1	−1	−1	−1	−1	−1	−1	−1	−1	−1	−1	−1	−1	−1	−1	−1	−1	−1	−1	−1	−1	−1	−1	−1

photometric probes around the scale model (one for the external illuminance and 9 for indoor illuminance values, placed according to the users' needs). After the acquisition of this data set, it is possible to obtain other building performance values only through calculation (e.g. work plane illuminance for other luminous conditions or other orientations).

3.2. Calculation procedure

For the measurement data to be interpreted, a matrix calculation has to be carried out. As the calculation is fully computerised, it no longer requires the scale model or the sky simulator.

The following calculation procedure is applied:

$$H\mathbf{f} = \mathbf{r} \tag{10}$$

with H, (28×28) matrix of Hadamard composed of a first column of (+1) and the following 27 as described in Table 2; $\mathbf{f}$, (28×1) vector of unknown factors (f_0: average value of the 27 factors, f_1 to f_{25}: illuminance due to the 25 skydome light sources, f_{26} and f_{27}: non assigned factors); $\mathbf{r}$, (28×1) responses vector (illuminance measurements of one photometer for the 28 experiments).

The two terms of Eq. (10) are multiplied by the transposed Hadamard matrix:

$$H^t H\mathbf{f} = H^t\mathbf{r} \tag{11}$$

With the Hadamard matrix property described in Eq. (A.1), it is possible to write:

$$n \cdot I_n \mathbf{f} = H^t\mathbf{r} \Rightarrow \mathbf{f} = \frac{1}{n} \cdot H^t r \tag{12}$$

with n, number of experiments ($n=28$); I_n, (28×28) identity matrix.

The vector $\mathbf{f}$ obtained this way allows the evaluation of the partial illuminance at a given point of measurement due to the 25 luminous zones of a given sky vault sector. As shown in the previous paragraph, the experimental plan is repeated six times (the scale model is rotated 60° at each step); therefore the matrix calculation is also repeated six times. Moreover, this calculation has to be executed for all photometers inside the scale model and for the external one used to assess external horizontal illuminance (reference probe). The indexes of $\mathbf{f}$ and $\mathbf{r}$ vectors are consequently chosen as follows:

$$\mathbf{f}^{p,s} = \begin{pmatrix} f_0^{p,s} \\ \vdots \\ f_m^{p,s} \\ \vdots \\ f_{27}^{p,s} \end{pmatrix} \quad \text{and} \quad \mathbf{r}^{p,s} = \begin{pmatrix} r_0^{p,s} \\ \vdots \\ r_m^{p,s} \\ \vdots \\ r_{27}^{p,s} \end{pmatrix} \tag{13}$$

with p, subscript of photometer number ($p=0$ for the probe placed horizontally outside the scale model); s, subscript of sky sector number ($s=1,\ldots,6$); f_m, factor number m with $m=0$: average of all factors (responses), $m=1,\ldots,25$ corresponding to the 25 scanning sky simulator light sources, $m=26$, 27: non-assigned factors (includes experimental errors); r_m measurement response from experiment number m.

By definition, the factors $f_m (m=1,\ldots,25)$, calculated by Hadamard's experiment design, correspond to the average illuminance due to the source number m operating in the two status on (+1) and off (−1).

As the partial illuminance is proportional to the light flux of source, f_m corresponds to a 50% lit lamp. The partial illuminance due to a light source m at full power is, in consequence, given by:

$$Ee_j = 2 \cdot f_m^{0,s} \quad \text{and} \quad Ei_j^p = 2 \cdot f_m^{p,s} \tag{14}$$

with m, s, j, lamp number m of sky sector number s corresponding to Tregenza's zone number j (see Fig. 4); Ee, external horizontal illuminance [Lx]; Ei^p, internal illuminance evaluated for photometer number p [Lx].

Thus, all quantities defined in Section 2 can easily be determined for all luminance distributions L_j.

In particular D_j evaluated at a given photometer position ρ, which is independent of the sky luminance distribution, can be written as:

$$D_j^p = \frac{Ei_j^p}{Ee_j} = \frac{f_m^{p,s}}{f_m^{0,s}} \tag{15}$$

A piece of software with a user-friendly graphical interface was developed to automatically analyse the data acquired with the scanning sky simulator. The main features of this software are the following:

- evaluation of the daylighting performance indicators defined in Section 2, namely:
  - Partial Daylight Factor (for all 145 different sky zones)
  - Partial Illuminance Factor (normalised for isotropic sky)
  - Illuminance Factor (for all CIE standard skies and monitored statistical skies)
  - Temporal Fraction of Satisfaction (assessed for Western Switzerland using IDMP data of Geneva (Ineichen and Molineaux, 1992))
- simulation of virtual orientation: Daylighting performance can be evaluated for different model orientations with angles that are multiples of the 60° angle

- taking into account a circumsolar component: A direct component of daylight can be added to a CIE standard sky (see Michel, 1999) to take into account specific meteorological situations
- taking into account window transmission coefficients: A multiplier factor can be applied to take into account the attenuation of the daylight flux through a window pane (if not reproduced on the scale model)
- taking into account an obstructed horizon: Different attenuation coefficients can be attributed to the 145 sky zones to simulate an obstructed horizon
- taking into account virtual mobile solar blinds: This functionality allows evaluating the daylight performance of a room from two measurement data sets: one 'with' direct sunlight, corresponding to an absence of solar blinds, the other 'without' direct sunlight. The calculation used to evaluate the TFS switches between the two situations according to a given rule that takes visual comfort into account, for instance 'solar blind closed' if the external horizontal illuminance exceeds 30 000 lux'.

3.3. Comparison of PDF assessment methods

A preliminary validation of the Hadamard experimental plan was carried out under the scanning sky simulator on the basis of the assessment of illuminance factors. The Illuminance Factor (IF) within a scale model of a room (height: 3 m; width: 3 m; length: 6.5 m) was measured for that purpose with the scanning sky simulator. Two experimental approaches were compared:

1. The Partial Daylight Factor (PDF) assessment method described above, which allows deter-

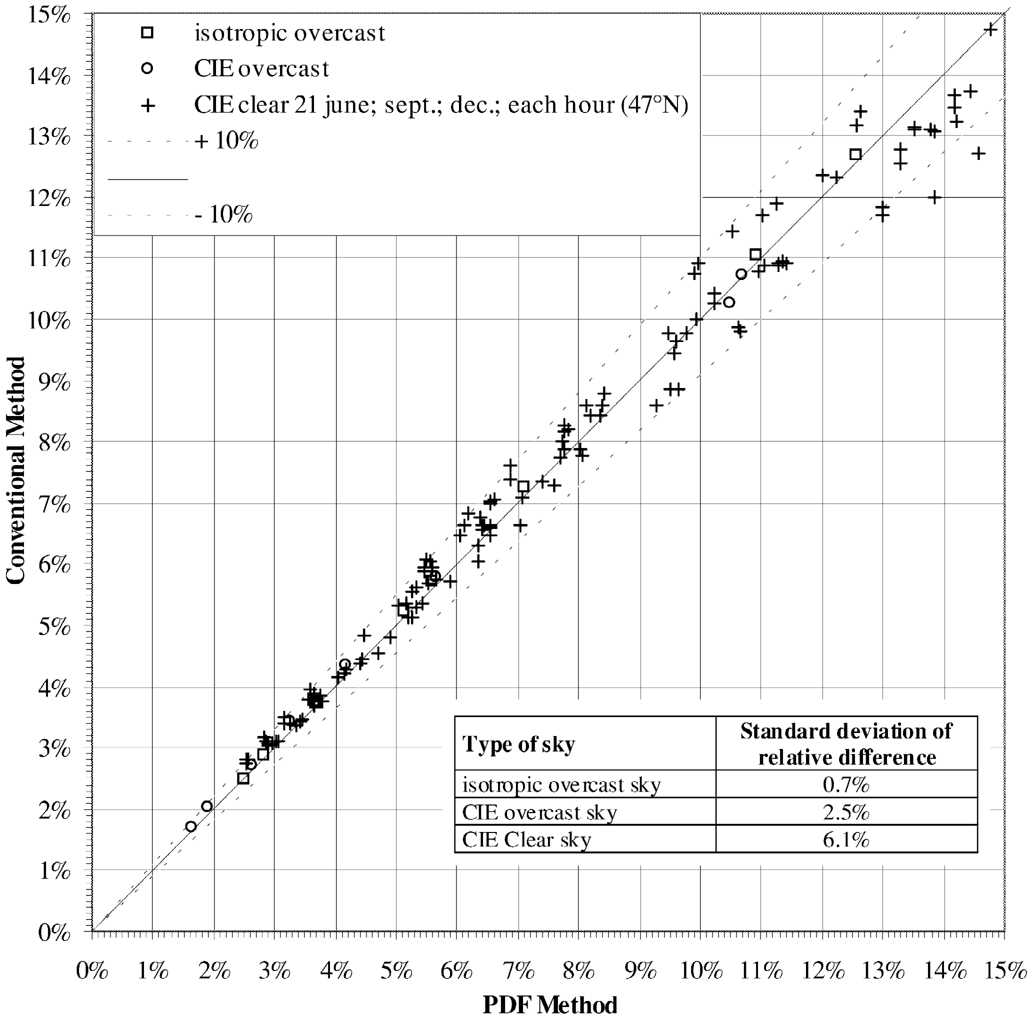

Fig. 6. Correlation of Illuminance Factor (IF) assessed with PDF experimental assessment method (Hadamard plan) vs. conventional operating mode of the scanning sky simulator.

mining IFs for any sky luminance distribution using a Hadamard experimental plan (set of 168 measurements that take about 20 min)
2. a standard IF assessment procedure (Michel *et al*., 1995) using the conventional operation mode of the scanning sky simulator, which allows a quicker and direct determination (in less than 2 min) of the IFs for a given sky luminance distribution

Twenty-two different sky luminance distributions were simulated using the scanning sky dome to achieve a statistically sound comparison of the two assessment methods. The following sky configurations were contained in this set:

- CIE standard and isotropic overcast skies
- CIE standard clear skies at winter solstice (8, 10 AM/noon/2, 4 PM), the equinoxes (6, 8, 10 AM/noon/2, 4, 6 PM) and summer solstice (5, 6, 8, 10 AM/noon/2, 4, 6 PM).

Fig. 6 illustrates the good concordance observed between the two assessment methods on a correlation diagram of their respective IF values. It appears, moreover, that sky luminance distributions characterised by rather low dynamics, such as overcast skies, lead to the best concordance between the two methods.

It follows that the PDF experimental assessment method based on the Hadamard experimen-

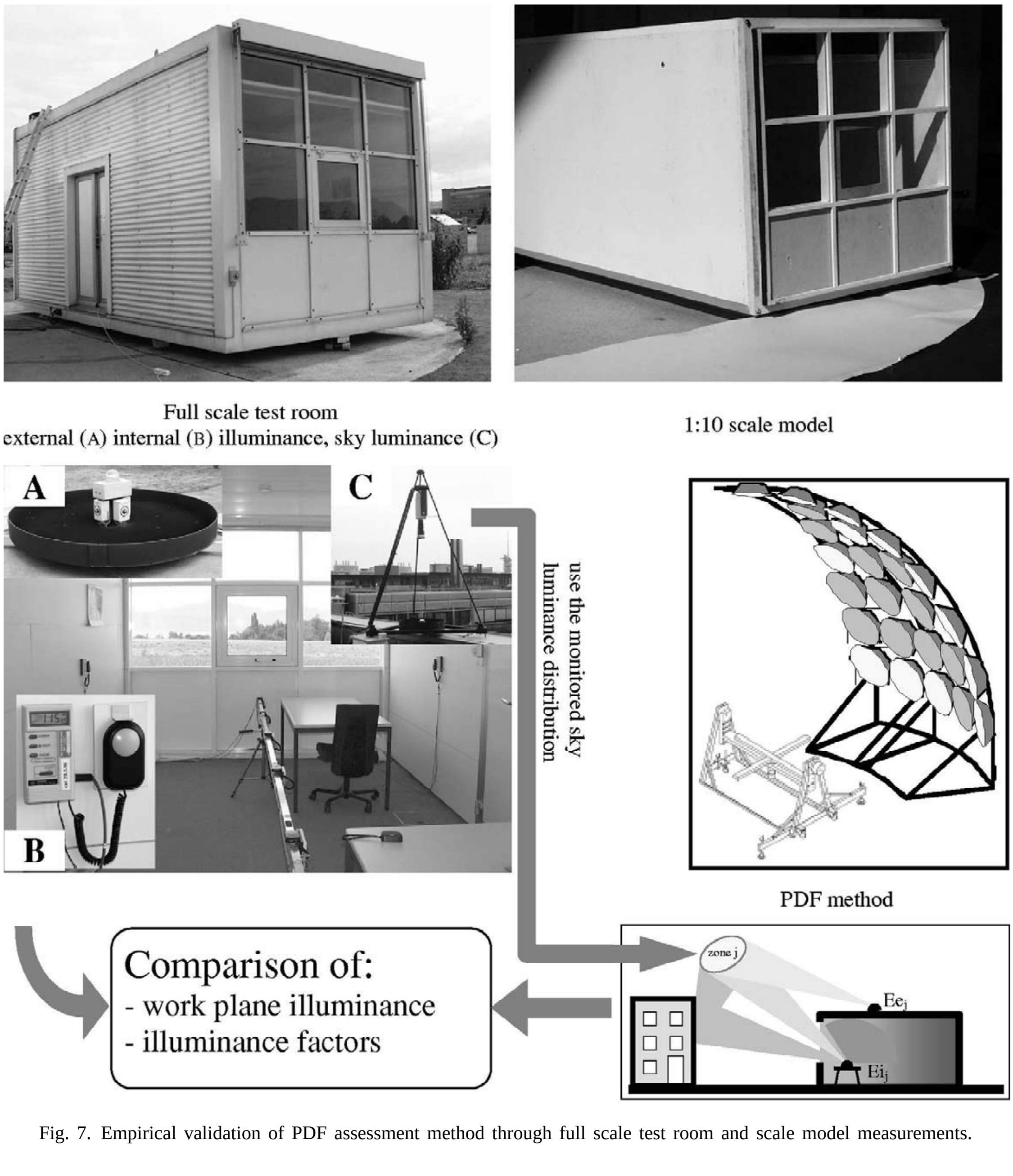

Fig. 7. Empirical validation of PDF assessment method through full scale test room and scale model measurements.

tal plan can be considered appropriate for the determination of IFs for any sky luminance distribution. Moreover, the the Hadamard experimental plan offers a better experimental accuracy than the conventional operation mode of the sky simulator by reducing the standard deviation of the estimated factor by $\sqrt{28} = 5.3$.

4. EMPIRICAL VALIDATION OF PDF ASSESSMENT METHOD

4.1. Description of experimental setup

A full-scale test room (3×3×6.5 m), located on the EPFL campus and mocking up an office room, (see Fig. 7 left), was used together with its corresponding 1:10 scale model to perform an empirical validation of the PDF assessment method. Table 3 gives the principal parameters of the test room; Fig. 15 (upper left) shows its cross section.

Work-plane illuminance profiles perpendicular to the window opening were monitored together with the external horizontal illuminance every five minutes for different winter meteorological conditions (clear, intermediate and overcast skies). A sky scanner, based on digital video imaging techniques and developed for that purpose (Michel, 1999; Michel and Andersen, 1999), was used to assess the 145 different IDMP average luminance values of the corresponding sky zones, showing a luminance dynamic range up to 75 dB for clear skies.

A 1:10 scale model of the test room was used in parallel to assess the PDF, using the Hadamard experimental plan described in Section 3.1, underneath the scanning sky simulator.

The daylighting performance indicators evaluated with this method were compared to the monitored ones in order to validate the novel experimental procedure.

4.2. Validation results

Different daylighting performance indicators were considered for different meteorological conditions, including the Daylight Factor (overcast sky), the Illuminance Factor (clear sky) and the work plane illuminance at different points in the room.

4.3. Overcast sky

Fig. 8 shows a comparison of Daylight Factors obtained with two different sky simulator operating procedures (CIE conventional and PDF method) and monitoring within the full scale rooms.

The average relative difference ΔIF% [see Eq. (16)] was used to compare the monitoring and the scale model figures together with the standard deviation. The same equation can be used to define the relative difference ΔDF% for daylight factors, considering only overcast sky conditions.

$$\Delta\text{IF\%} = \frac{\text{IF}_{\text{PDF}} - \text{IF}_{\text{real}}}{\text{IF}_{\text{real}}} = \frac{Ei_{\text{PDF}} - Ei_{\text{real}}}{Ei_{\text{real}}}\,[-] \quad (16)$$

with IF_{real}, Illuminance Factor monitored in the full scale test room [–]; IF_{PDF}, Illuminance Factor evaluated using the PDF method within the scanning sky simulator [–]; Ei_{real}, work plane illuminance monitored in the full scale test room [Lx]; E_{PDF}, work plane illuminance evaluated using the PDF method with the scanning sky simulator [Lx].

The analysis of Fig. 8 and Table 4 leads to the following conclusions:

- as the PDF method uses the monitored sky luminance distributions, it allows a more accurate evaluation of Daylight Factors than the CIE standard method. Since there is an unavoidable difference between the effective and the Moon and Spencer sky luminance distribution, this can also be verified for overcast skies.

Table 3. Main features of the full-scale test room and corresponding 1:10 scale model

Parameters	Full-scale test room	1:10 scale model
Side wall reflectance	0.81	0.83
Back wall reflectance	0.73	0.73
Ceiling reflectance	0.81	0.83
Internal ground reflectance	0.16	0.17
Nearby external ground reflectance	0.38	0.43
Distant external ground reflectance	0.06–0.10	0.05
Double glazing transmittance	0.80 (glass)	0.85 (plastic)
Dimensions errors	±1 cm	± 1 mm
Horizon	unobstructed: <5°	unobstructed: 0°
Orientation	South (±5°)	South (±1°)

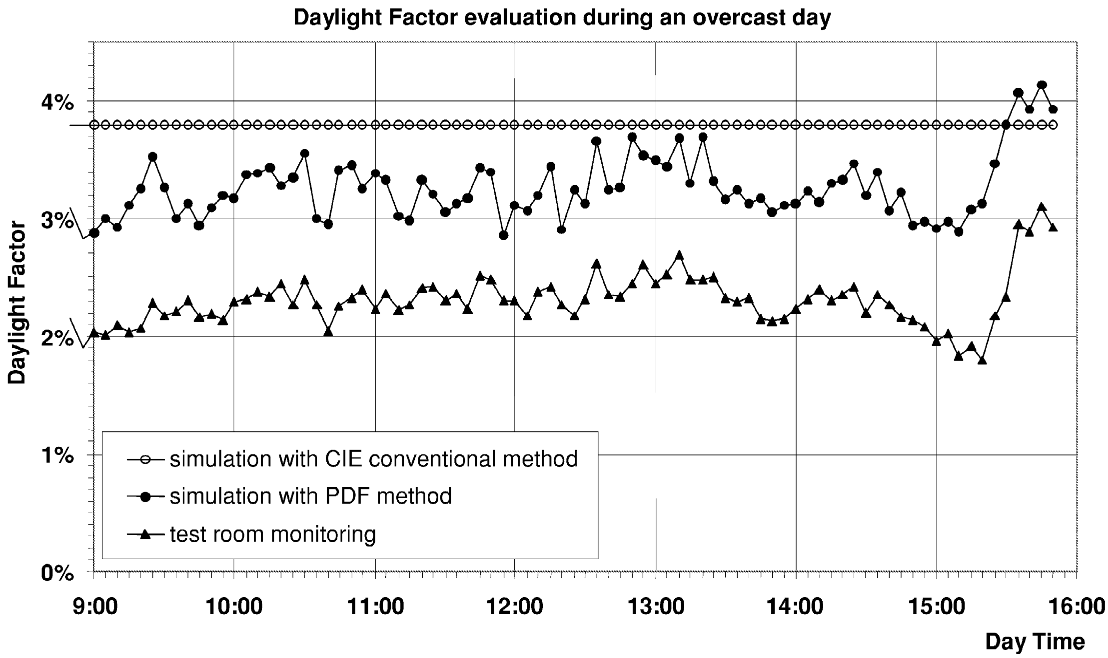

Fig. 8. Comparison of Daylight Factors obtained through full-scale test room monitoring and different sky simulator operating procedures (CIE conventional and PDF method).

- The standard deviation of the relative difference DF% for the PDF method is comparable to experimental relative errors (estimated between 5 and 8%).
- There are several explanations for the difference between monitored results and those obtained through the PDF method underneath the sky simulator, namely:
  - the construction differences between the full scale test room and the 1:10 scale model (size, surface properties, glazing)
  - the horizon error within the sky simulator
  - the experimental errors during the test room monitoring (photometric correction of sensors, cosine errors, etc.)

Despite the systematic difference between monitored figures and those assessed with the PDF method, it is believed that a significant improvement is achieved in the accuracy of the DF or IF assessment compared to a CIE standard approach.

4.4. Clear sky

The clear sky situation (south orientation, winter conditions in Switzerland) chosen to compare the PDF method and monitoring results is one of the most critical, as direct sunlight penetrates deep into the room and causes very sharp shadows. It is therefore well suited to illustrate the advantages and limits of the PDF method.

Illuminance values monitored on the work plane at different distances from the window inside the full scale test room and in the scale model lead to the following observations:

- The vertical window frames shadowing the work plane at a distance of 2.25 m from the opening (see Fig. 9) is responsible for large illuminance variations; the PDF method is not able to reproduce such sharp shadow effects, since an expanded light source, such as the one designed for the sky simulator (see Fig. 11) produces penumbra.
- Deeper into the room, at a distance of 5.25 m from the window (see Fig. 10), the PDF method significantly overestimates the work plane illuminance. As shown in Fig. 12, the finite dimension of the circular light sources of the sky simulator (which sustain a 10° angular sector from the skydome centre) is responsible

Table 4. Average value and standard deviation of relative difference of Daylight Factors (DF) assessed using full scale test room monitoring and PDF method

	Average value	Standard deviation
CIE conventional method	67%	16%
PDF method	42%	8%

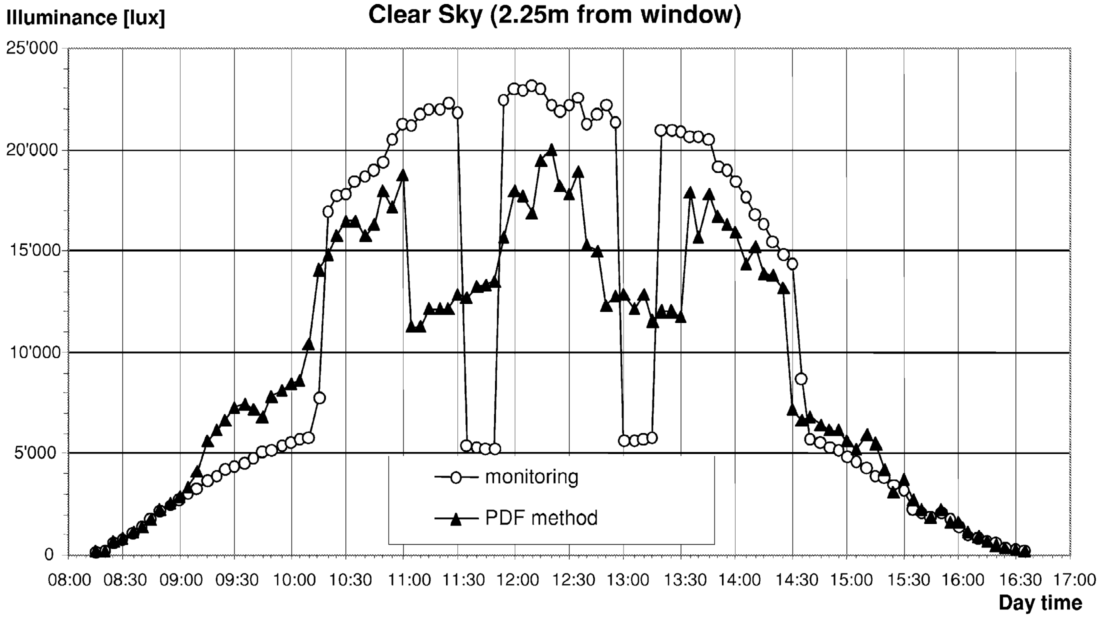

Fig. 9. Work plane illuminance observed during a whole winter sunny day (8 December, Switzerland) at 2.25 m from the window through full scale monitoring and PDF method underneath the sky simulator.

for this situation, as the direct sunlight originates from a point source that in some cases is totally obstructed by obstacles (such as window frames and mullions).

One realizes in consequence that the partition of the sky vault into 145 light sources of finite dimensions is responsible for significant discrepancies with regard to the monitoring results, as could be expected from the PDF method assessment procedure. By grouping different sensors in order to average work plane illuminances in given room areas, a significant improvement of

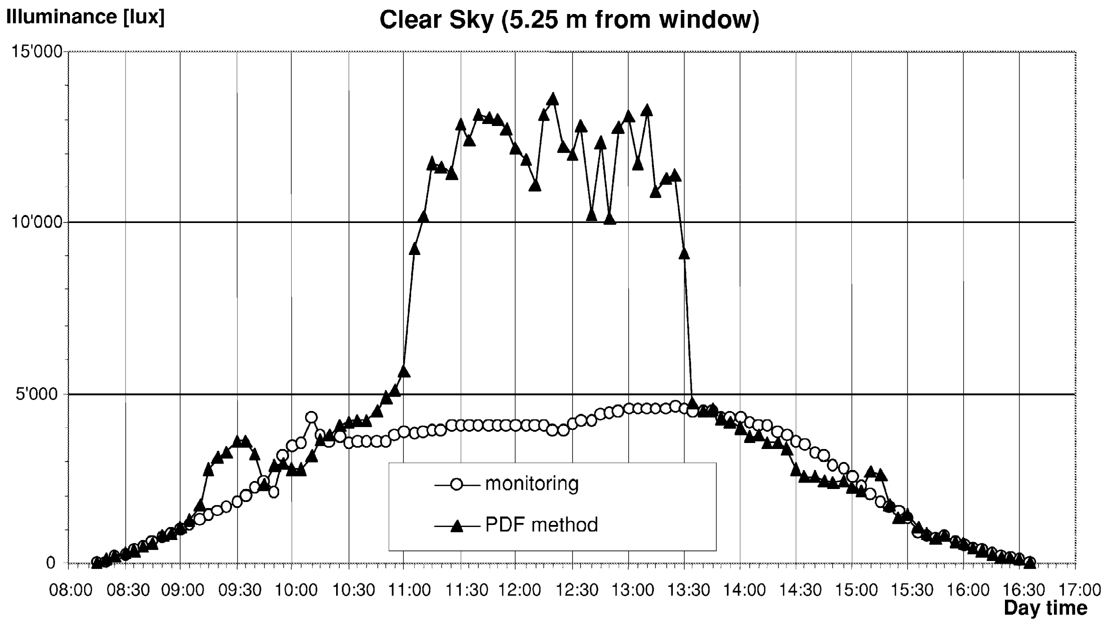

Fig. 10. Work plane illuminance observed during a whole winter sunny day (8 December, Switzerland) at 5.25 m from the window through full scale monitoring and PDF method under the sky simulator.

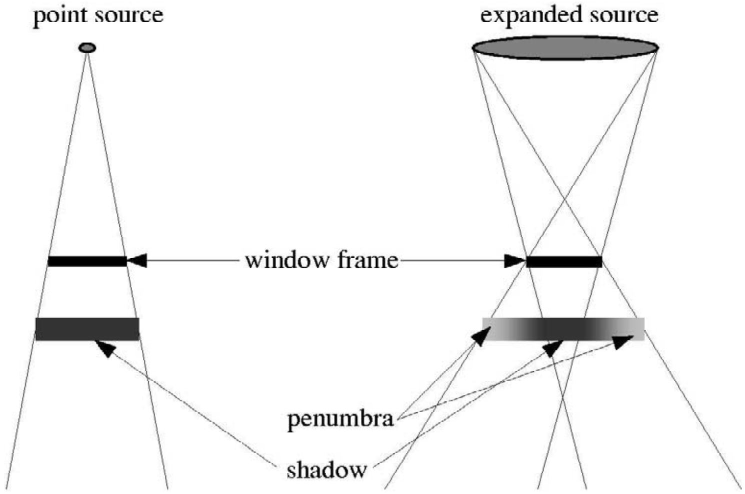

Fig. 11. Illustration of the shadowing effect due to a spot and an expanded light source.

this situation can be achieved. The following area and corresponding illuminance sensors were considered for that purpose:

- probes located at 1.25, 2.25 and 3.25 m from the window were lumped together to assess the average illuminance near the window (see Fig. 13)
- probes located at 4.25, 5.25 and 6.25 m from the window were lumped together to assess the average illuminance at the back of the room (see Fig. 14)

The following observations can be drawn from the comparison of the average work plane illuminance assessed with the two different methods:

- the standard deviation of the relative illuminance difference is worth 15% and 30% respectively, leading to discrepancies higher than the one observed for overcast skies, very reasonable, however, when taking into account the dynamics of work plane illuminance under clear skies (variation of a factor 1 to 5)
- the shadowing effect of the window frame and mullion is almost not visible any more, since the fact of considering the average illuminance of a given finite room area significantly improves the agreement between the PDF method and monitored figures; however, one has to give up the possibility to perceive the shadowing effects related to window frames

5. APPLICATION OF THE PDF METHOD

The PDF method was applied to assess the daylighting performance of a novel daylighting system, an anidolic ceiling (Courret *et al.*, 1998; Courret, 1999) in comparison to a conventional double glazing facade (considered as the reference facade).

The system consists of a light duct, integrated into a suspended ceiling and leading midway into an office room. Anidolic (non-imaging) optical devices are placed on either end of the duct, on

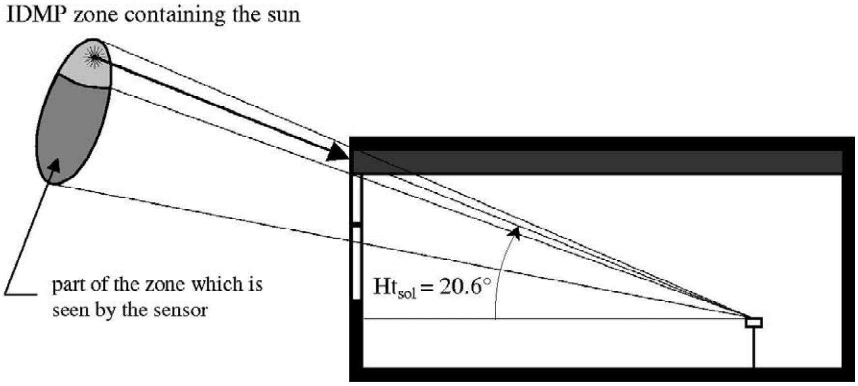

Fig. 12. Illustration of the situation where the direct sunlight does not reach a sensor, that ‘sees’ a large part of the IDMP lighting zone which includes the sun.

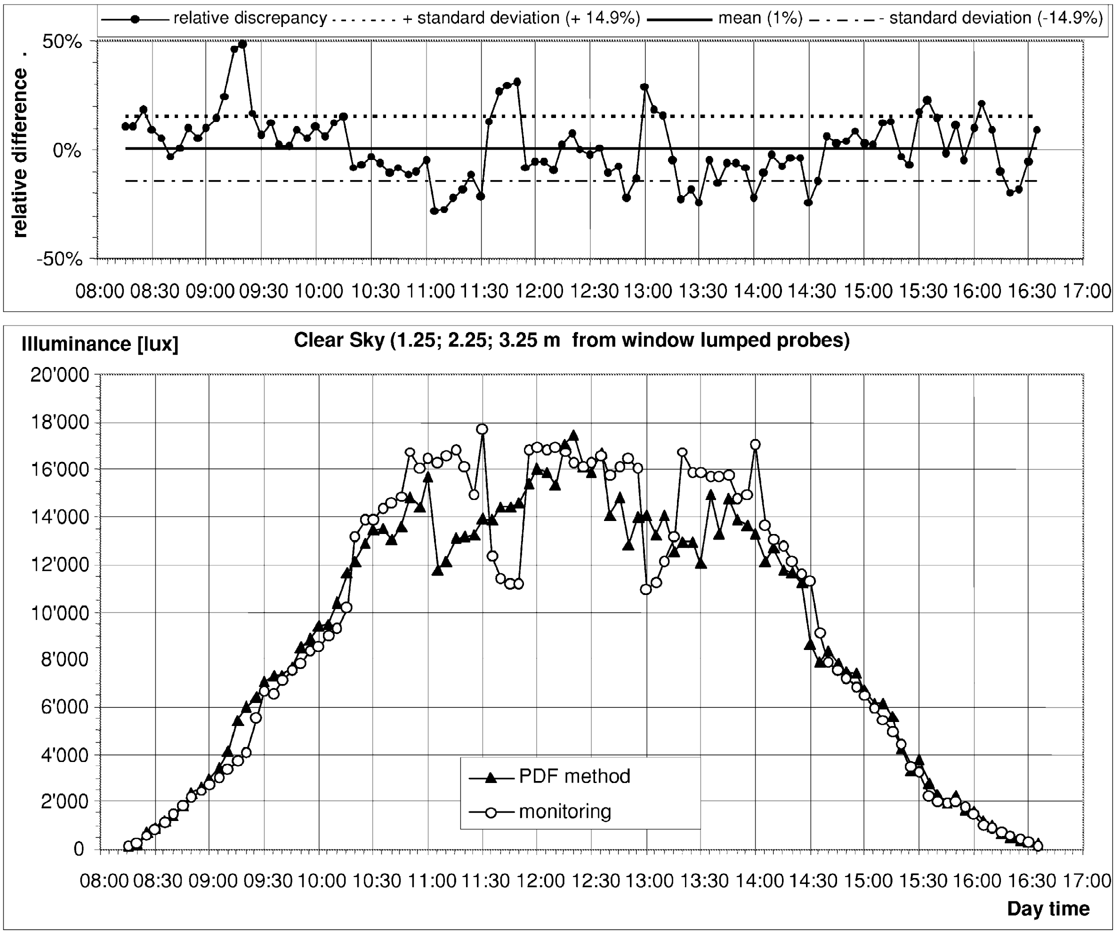

Fig. 13. Lower graph: Average illuminance in the front part of the room (1.25, 2.25 and 3.25 m from window). Upper graph: Relative discrepancy between the PDF method and monitored figures.

the outside to collect light rays from the sky vault and on the inside to control the direction of the emitted light flux. Outside the facade, a concentrator bundles daylight from the upper area of the sky vault, which is usually brighter with overcast skies. At the exit aperture of the duct, a compound parabolic reflector distributes the light flux downwards without any backward reflection. Thanks to this feature, visual comfort is improved in comparison to window integrated daylighting systems. An external solar blind is installed to control direct penetration of sunlight through the device and thus to reduce over-heating and glare risks. Anidolic ceilings can be used in rural areas: their effect is, however, more pronounced in urban areas where obstructions reduce the contribution of the lower part of the sky vault to the daylighting of a room.

Fig. 15 shows a schematic view of the full scale anidolic ceiling test room together with the associated reference (double glazing facade).

Fig. 16 illustrates the DF profiles assessed with the PDF method under the sky simulator for the novel daylighting system and the reference facade, using 1:10 scale models of the two different rooms. It appears that a significant improvement of the Daylight Factor can be achieved by the anidolic ceiling in the deeper part of the room (DF>5% instead of 2% in the range of 4–5 m from the window).

The Temporal Fraction of Satisfaction (TFS) profiles with regard to daylight sufficiency were determined for the two different rooms using the PDF method. They show a significant energy savings potential, estimated at 30% in comparison to the reference facade, due to this novel device (see Fig. 17). A similar analysis could be made using the other two criteria used to define the TFS lighting requirements as described in Section 2.

The Partial Illuminance Factor (PIF) at a distance of 4.25 m from the window (see Fig. 18), represented through a stereographic projection, leads to the following analysis:

- the anidolic ceiling expands the fraction of the

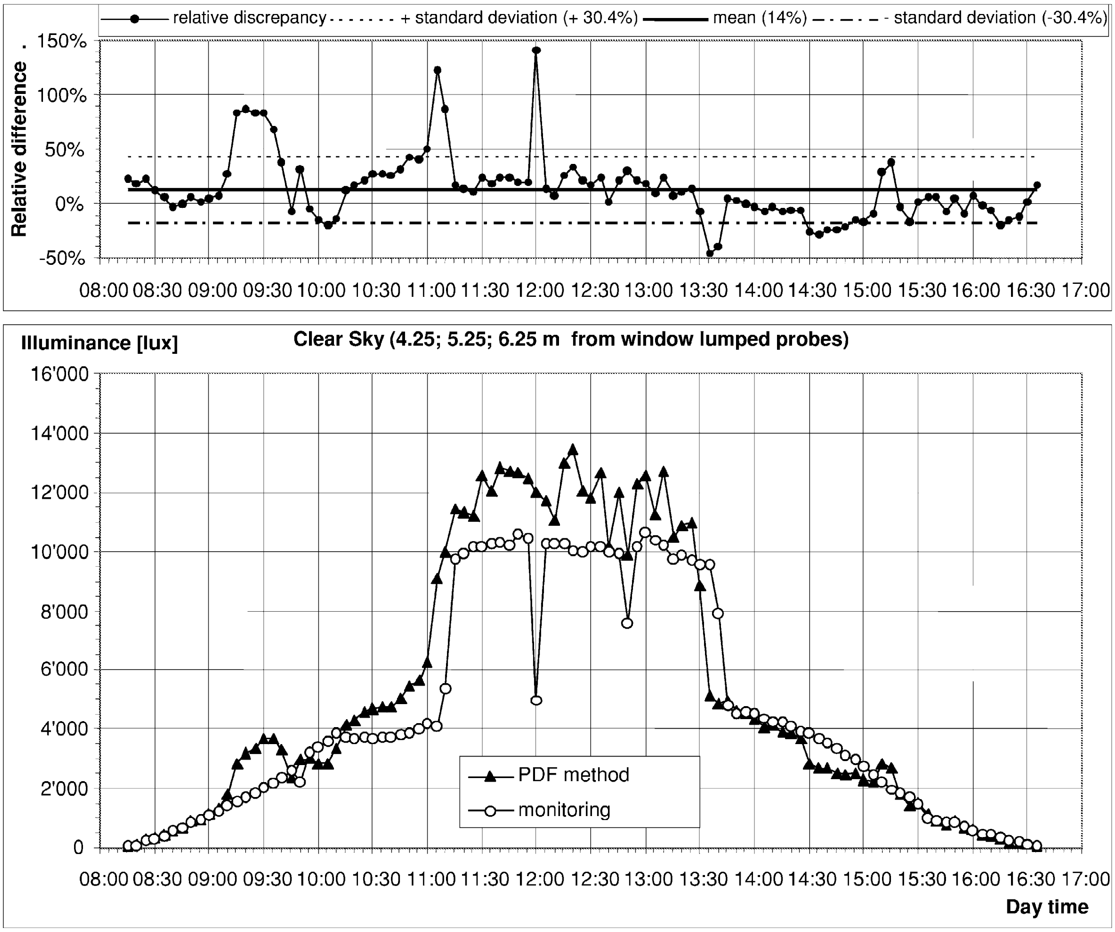

Fig. 14. Lower graph: Average illuminance in the rear part of the room (4.25, 5.25 and 6.25 m from the window gathered probes). Upper graph: Relative discrepancy between the PDF method and monitored figures.

sky vault that contributes to the work plane illuminance in the room, which explains the higher performance achieved by the novel device

- the superimposed sun paths for solstices and equinoxes give an indication of the potential glare risks of the system due to direct sunlight penetration. For the anidolic ceiling, the summer sun path crosses sky zones that significantly contribute to the work plane illuminance, which makes it necessary to install solar blinds on the external anidolic collector.

6. CONCLUSION

The PDF method applied to a scanning sky simulator that works with scale models was compared with figures monitored in full scale test rooms for some representative weather situations (overcast, intermediate and clear skies). The method was used to assess several daylighting performance indicators, such as Illuminance Factors (IF), Partial Illuminance Factors (PIF) and Temporal Fractions of Satisfaction (TFS), which are key figures for the appraisal of buildings and daylighting systems in research and practice. The good agreement between the figures shows that even in delicate cases, characterised by winter sunlight penetration, the PDF method allows a sound and accurate evaluation of the luminous performance of a building based on these indicators.

An experimental study (Cannon-Brookes, 1997) dedicated to the evaluation of the sources of error within a scale model, showed that the measurements performed in such a scale model and those monitored on-site lead to relative discrepancies of up to 20%. The results presented in this paper show a comparable experimental agreement and thus corroborate the conclusions of

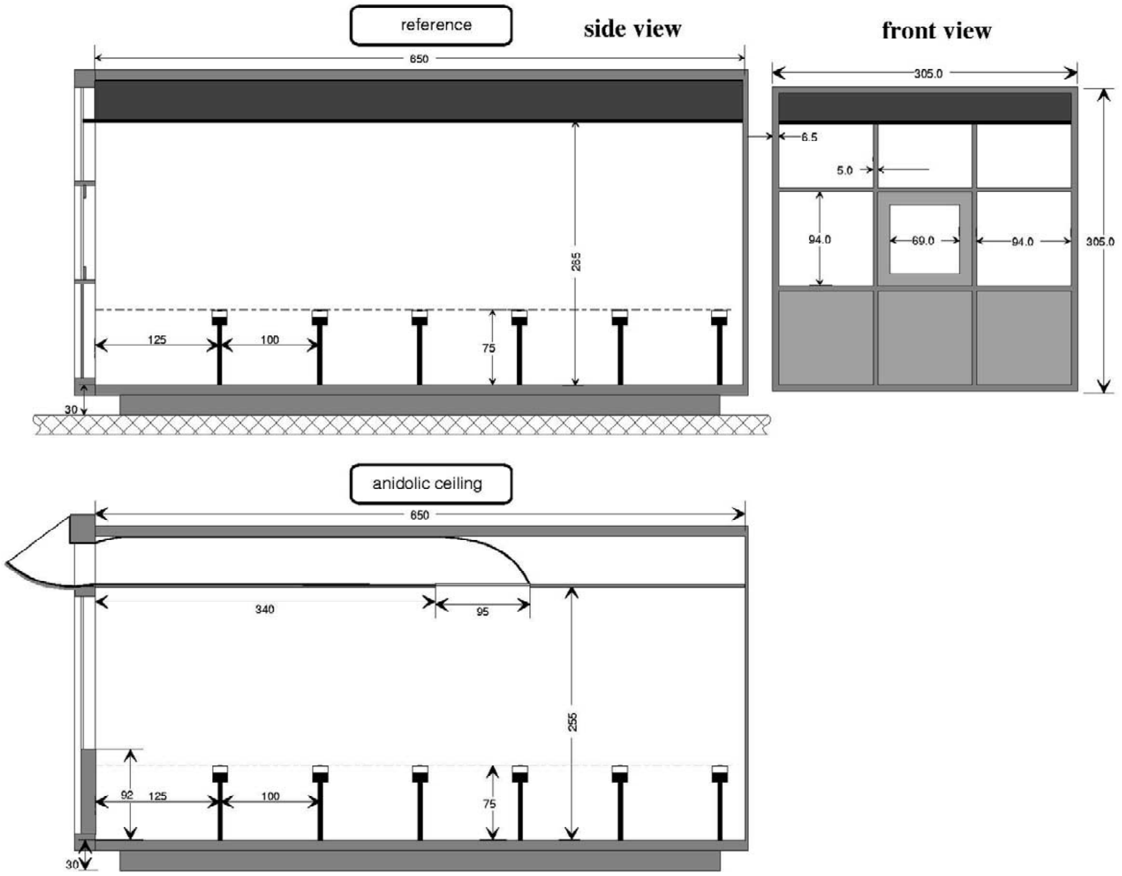

Fig. 15. Schematic view of the full scale anidolic ceiling test room and the corresponding reference facade (double glazing facade).

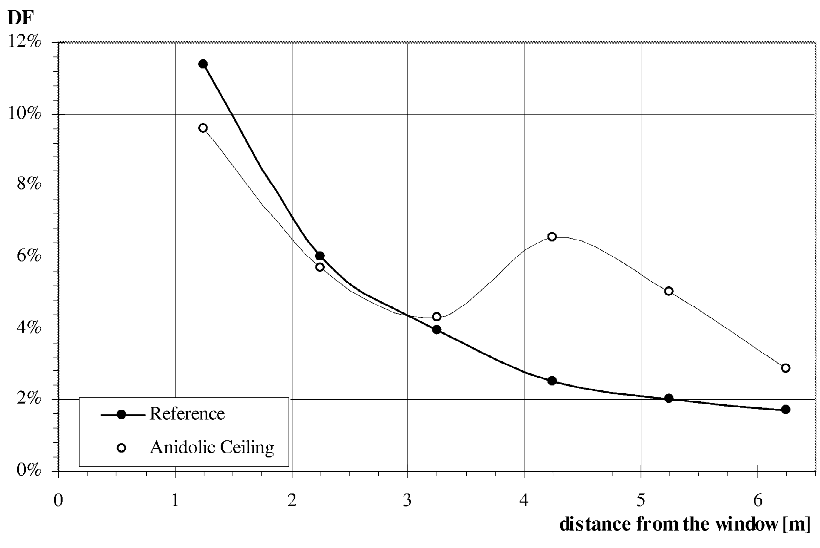

Fig. 16. Daylight Factor Profile assessed for the anidolic ceiling and the reference facade (double glazing facade) through the PDF method.

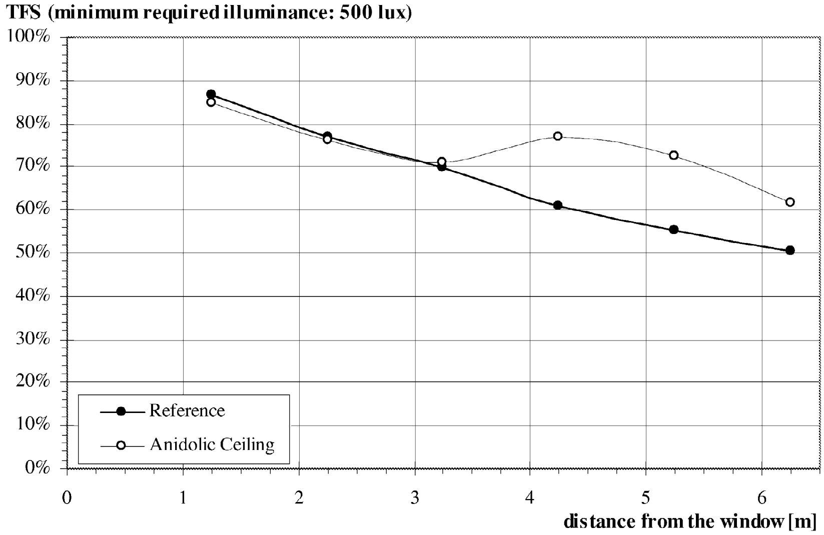

Fig. 17. Temporal Fraction of Satisfaction (TFS) profile assessed for the anidolic ceiling and the reference room through the PDF method; corresponds in this case to the relative fraction of annual working hours (from 8 AM to 6 PM local time without daylight saving hours), that benefit from sufficient work plane illuminance through daylight (500 lux required illuminance).

Cannon-Brookes. One can therefore affirm that the PDF method generally does not produce larger discrepancies with regard to on-site monitored figures than those induced by the scale models themselves.

One of the main limitations of the method is, however, that shadowing effects due to window frames when direct sun light penetrates into the room cannot be reproduced. Indeed, the method, which is based on 145 luminous zones of finite dimensions, does not allow highlighting the consequences of a strong heterogeneity of luminance within a corresponding (10°) angular sector.

However, numerous applications of the PDF method, which will benefit building and lighting designers, demonstrate the usefulness of the method for the assessment of the daylighting performance of buildings.

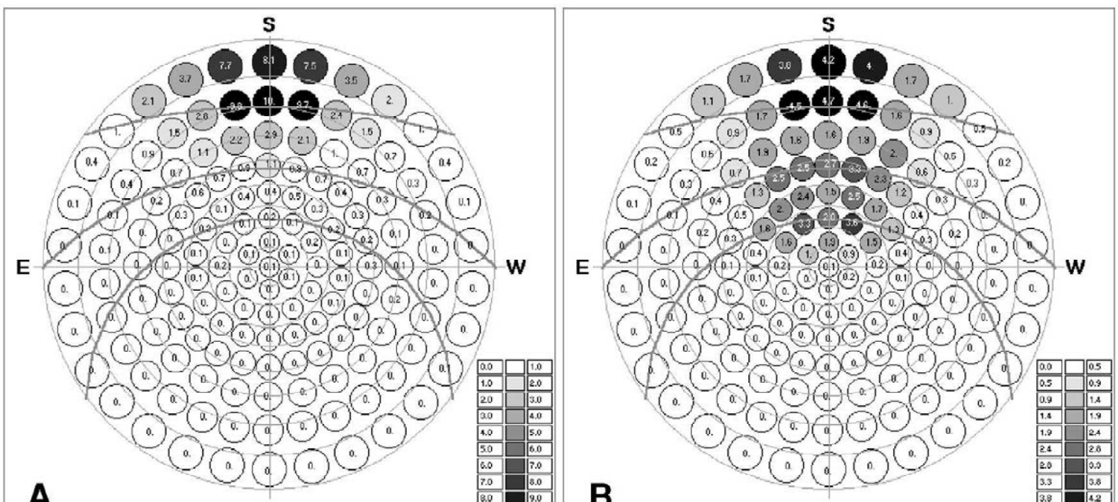

Fig. 18. Stereographic projections of Partial Illuminance Factor (PIF, given in %) for reference facade (A) and anidolic ceiling (B) at a distance of 4.25 m from the window. Sun paths (solstices and equinox) for 47°N latitude are superimposed.

NOMENCLATURE

D_j [–]	Partial Daylight Factor at a given building internal point due to the contribution of luminous zone j of the sky vault
Ei_j [Lx]	Contribution of luminous zone j of the sky vault to the work plane illuminance at a given building internal point
Ee_j [Lx]	Contribution of luminous zone j of the sky vault to the external horizontal illuminance
L_j [cd/m2]	Average luminance of luminous zone j of the sky vault
Ω_j [sr]	Apparent solid angle of luminous zone j of the sky vault
η_j [rad]	Angular altitude of the centre of luminous zone j
Ee_0^{iso} [Lx]	External horizontal illuminance of an isotropic sky
Ee_j^{iso} [Lx]	Contribution of luminous zone j of an isotropic sky to the external horizontal illuminance
Ee_0 [Lx]	External horizontal illuminance observed for a certain luminance distribution (non isotropic)
L^{iso} [cd/m2]	Isotropic sky constant luminance
Ei_0 [Lx)]	Horizontal work plane illuminance at a given building internal point
IF [–]	Illuminance Factor at a given building internal point observed for a certain sky luminance distribution (overcast and non overcast)
DF [–]	Daylight Factor at a given building internal point observed for overcast sky conditions (Moon and Spencer luminance distribution)
L_z [cd/m2]	Zenithal sky luminance
PIF_j [–]	Partial Illuminance Factor at a given building internal point due to the contribution of luminous zone j of the sky vault
TFS [–]	Annual fraction of working hours during which the work plane illuminance at a given internal building point satisfies a certain lighting criterion
H	$(n \times n)$ Hadamard matrix associated to an $(n \times n)$ experimental plan
H^t	transposed matrix associated to an $(n \times n)$ Hadamard experimental plan number of experiments
I_n	$(n \times n)$ identity matrix
$\mathbf{f}$	$(n \times 1)$ vector of unknown factors of an experimental plan
$\mathbf{r}$	$(n \times 1)$ response vector of an experimental plan
ΔIF% [–]	Relative difference between monitored and by means of PDF method simulated Illuminance Factor
IF_{real} [–]	Full scale test room monitored Illuminance Factor
IF_{PDF} [–]	Simulated Illuminance Factor (PDF method)
Ei_{real} [Lx]	Full scale test room monitored work plane illuminance
Ei_{PDF} [Lx]	Simulated difference between monitored and by means of PDF method simulated Daylight Factor
ΔDF% [–]	Relative difference between monitored and by means of PDF method simulated Daylight Factor

APPENDIX A. EXPERIMENTAL PLAN USING HADAMARD MATRICES

It can be shown (Hedayat and Wallis, 1978) that a square matrix H of order n whose entries are $(+1)$ or (-1) is a *Hadamard matrix of order n*, provided that its rows are pairwise orthogonal. In other words:

$$H^t \cdot H = n \cdot I_n \tag{A.1}$$

with H, matrix associated to a $(n \times n)$ experiment design; H^t, transposed matrix associated to an $(n \times n)$ experiment design; n, number of experiments; I_n, $(n \times n)$ identity matrix. The system has to be exclusively additive and consequently without interaction. All of the associated matrix elements are $(+1)$ or (-1). The necessary (but not sufficient) criterion for the existence of such a matrix is that the experiment number n to evaluate $(n-1)$ factors is 2 or a multiple of 4.

The Cauchy–Schwarz inequality (see Eq. (A.2)) shows that the Hadamard experimental design, whose variance of each estimated factor is given by Eq. (A.3), is optimal. Thus, the Hadamard experimental design allows an efficient and optimal estimation of the principal effects of factors.

$$\text{Cauchy–Schwarz inequality:} \quad \mathrm{Var}(f_i) \geq \frac{\mathrm{Var}(m_i)}{n} \tag{A.2}$$

with $\mathrm{Var}(f_i)$, variance of the estimated factor f_i for any experimental plan; $\mathrm{Var}(m_i)$, variance of measurement result m_i of factor f_i.

The variance of estimator f_i through Hadamard experimental design is given by the following equation:

$$\mathrm{Var}(f_i) = \frac{\mathrm{Var}(m_i)}{n} \Rightarrow \sigma(f_i) = \frac{\sigma(m_i)}{\sqrt{n}} \tag{A.3}$$

with $\sigma(f_i)$, standard deviation of the estimated factor f_i; $\sigma(m_i)$, standard deviation of measurement result m_i of factor f_i.

REFERENCES

Cannon-Brookes S. W. A. (1997) Simple scale models for daylighting design: analysis of sources of error in illuminance prediction. *Lighting Res. Technol.* **29**(3), 135–142.

CIE16 (1970) Daylight, Commission Internationale de l'Eclairage (CIE), 16 (E-3.2), Paris.

Courret G. (1999) Systèmes anidoliques d'éclairage naturel. Thèse Doctorat No. 2026, Département d'Architecture, Ecole Polytechnique Fédérale de Lausanne (EPFL), Lausanne.

Courret G., Scartezzini J. -L., Francioli D. and Meyer J. -J. (1998) Design and assessment of an anidolic light-duct.

Energy and Buildings **28**, 79–99.

Dumortier D. (1995). *Mesure, Analyse Et Modélisation Du Gisement Lumineux. Application à l'Évaluation Des Performances De l'Éclairage Naturel Des Bâtiments*, Université de Savoie, France.

Hedayat A. and Wallis W. D. (1978) Hadamard matrices and their applications. *Annals Stat.* **6**(6), 1184–1238.

Ineichen P. and Molineaux B. (1992). *PRC Krochmann Sky Scanner Characterisation*, GAP-CUEPE, Genève.

Michel L. (1999) Méthode expérimentale d'évaluation des performances lumineuses de bâtiments. Thèse de Doctorat No. 2042, Département d'Architecture, Ecole Polytechnique Fédérale de Lausanne (EPFL), Lausanne

Michel L. and Andersen M. (1999) Réalisation d'un photo-uranotomographe à imagerie numérique. In *CISBAT'99*, pp. 289–294, EPFL, Lausanne.

Michel L., Roecker C. and Scartezzini J. -L. (1995) Performances of a new scanning sky simulator. *Lighting Res. Technol.* **27**(4), 197–207.

Papamichael K. and Beltran L. (1993). *Simulating the Daylight Performance of Fenestration Systems and Spaces of Arbitrary Complexity: The IDC Method*, Lawrence Berkeley Laboratory, Berkeley, California, USA.

Plackett R. L. and Burman J. P. (1946) The design of of optimum multifactorial experiments. *Biometrika* **33**(4), 305–325.

Tregenza P. R. (1980) The daylight factor and actual illuminance ratios. *Lighting Res. Technol.* **12**(2), 64–68.

Tregenza P. R. (1987) Subdivision of the sky hemisphere for luminance measurements. *Lighting Res. Technol.* **19**, 13–14.

Tregenza P. R. (1989) Daylight measurement in models: new type of equipment. *Lighting Res. Technol.* **21**(4), 193–194.

Tregenza P. R. and Waters I. M. (1983) Daylight coefficients. *Lighting Res. Technol.* **15**(2), 65–71.